Discrete Time Sliding Mode Control with Simple VSS Observer of Zero-Power Magnetic Bearing Systems

Kenzo Nonami and Kenichi Nishina

Dept. of Mechanical Engineering, Chiba University
1-33 Yayoi-cho, Inage-ku, Chiba 263, Japan
tel/fax +81-43-290-3195; e-mail nonami@meneth.tm.chiba-u.ac.jp

Abstract

This paper deals with the discrete time sliding mode control of a rotor-magnetic bearing system with zero power scheme using a permanent magnet. We propose a new actuator in which the flux circuit of the zero power scheme using a permanent magnet can be varied. A mathematical model of zero power sceme using permanent magnet and a flexible rotor is derived. The reduced-order model is described for the controller by eliminating higher-order modes of the mathematical and electrical magnet interation system beyond the fourth flexible mode. The sliding mode control system for reduced-order model is designed using the discrete time VSS observer. The simulations are done for the two cases of lift off and rotations. The two unstable rigid modes can be easily controlled with good stability, and the spillover phenomena of the higher-order modes are not generated. It is also clear that the proposed discrete time sliding mode controller has robustness against model parameter variations and external disturbances, compared with the conventional control methods like PID control and disturbance cancellation control.

1 Introduction

The "dream" of supporting an object on a non-contact basis has existed for a long time. The most important object of this is to gain freedom from lubrication and mechanical friction that necessarily accompany contact, thereby completely nullifying the energy loss which has been an obstacle of high-speed operations and fast rotations. This "dream" was attempted, at an initial stage, as levitation by means of only a permanent magnet. This was shown by Earnshaw to be impossible. Thus, the magnetic levitation and magnetic bearing technology became deeply intertwined with control theory to such an extend that it became a field which contributed positively to control theory as a typical model of the stabilization control of unstable systems.

Several years have already passed since magnetic bearing control systems were put into practical use, but almost all these systems are small rotational machines as represented by turbo molecular pumps. These have common points in terms of bearing rigid rotors, having analog PID control, and being active magnetic bearings based on 5-axis control type attractive systems in most cases. With these achievements in the background, the expectation for magnetic bearing systems has increased to an even higher degree, with the result that studies and developmental work on technology for higher performance are being carried out. In particular, some of the recent research subjects and topics[1]-[4] may be listed as follows: (1) Studies on shifts from the conventional analog control to digital control using digital signal processors. (DSPs); (2) Studies on shifts from the stabilization control of PID control to advanced control in which modern control theory, robust control theory, and learning control, as well as design methods, such as control systems with disturbance compensation, are applied; (3) Studies of flexible rotor and magnetic bearing control systems which pass higher-order flexible modes;(4) Studies of sensorless magnetic bearings for estimating and controlling rotor displacements from the currents of magnetizing coils by the use of observer theories and others or for using PWM carrier frequency waves; (5) Studies for the joint use of electromagnets as magnetic bearings for levitation control and also as motor stators for rotation control; (6) Studies of zero-power type magnetic bearings for energy savings in which permanent magnet and electromagnets are jointly used;(7) Studies of superconducting magnetic bearings which possess high rigidity and high load; (8) Studies of power amplifier and actuator design for realizing ultra-high-speed rotations; (9) Studies for increasing reliability by the elucidation of non-linear phenomena in magnetic fields or the elucidation of transient phenomena during touch downs in emergencies; (10) Studies of test results for applications to actual machines and for attempts at applications to new fields.

One of the author has been aggressively carrying out to apply the latest advanced control theory for magnetic bearing control[5]-[9]. In particular, it is confirmed for us that sliding mode control as nonlinear control strategy is very useful for magnetic bearing system[10]-[11]. This paper is concerned with not only (1),(2) but also (6). The bias attractive force of the electromagnet using a bias current is replaced by the attractive force of the permanent magnet to save an energy. The electomagnet is used for only active control. We propose a new type zero-power magnetic bearing system using permanet magnet which can vary attractive force. Therefore, it becomes very easy to tune a controller because of variable bias attractive force. Also, we propose a convenient and sipmle discrete time sliding mode control system design with VSS observer for magnetic bearing control.

2 Zero-Power Magnetic Bearing Systems

2.1 Concept of Zero-Power Magnetic Bearing

Figure 1 shows the concept of zero-power magnetic bearing system. The actuator consists of a permanent magnet and a electoromagnet as a hybrid magnet. The steady-state attractive force is provided by a permanent magnet and the control attractive force is supplied by electromagnets. It is easy to change a attractive force of permanent magnet. So, all of the steady-state attractive force can be provided by only permanent magnet or some ratio of it is provided by electromagnet. This is the most original zero-power magnetic bearing.

The adjustment of the attractive force is carried out by a adjusment screw as shown in Fig.1. The flux path of the magnetic circuit in the case of zero-gap between the permanent magnet and the head of the screw. The attractive force for the rotor is almost zero in such case. On the contrary, the flux path is b in the case of a big-gap. In that case, the maximum attractive force arises for the rotor. Figure 2 shows the relation between the attractive force and the gap of permanent magnet. It is a strong nonlinear characteristics.

2.2 Test Rig

Figure 3 shows the cross-sectional view of the experimental setup of zero-power magnetic bearing system. The four radial magnetic bearings are provided by a zero-power magnetic bearing and a couple of repulsive permanet magnet without control is used for a axial magnetic bearing. The high frequency motor is installed at the middle of the rotor. The rotor will be completely non-contact levitated with control. An optical sensors are used for measurements of the rotor displacements to avoid an interation with magnetic field.

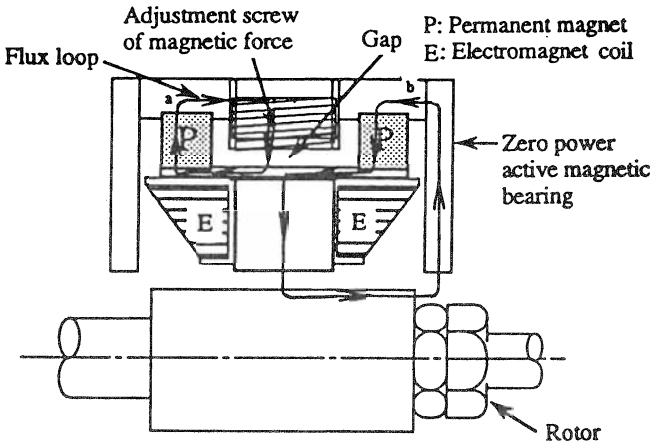

Fig. 1 Concept of zero-power magnetic bearing

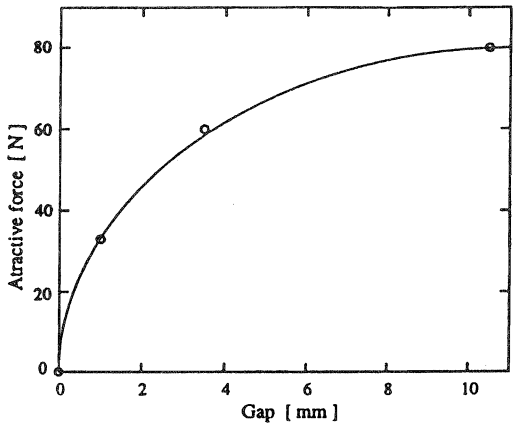

Fig. 2 Relation between attractive force and gap of permanent magnet

3 Modeling of Flexible Rotors / Zero-Power Magnetic Bearing Systems

3.1 Modeling of Magnetic Bearing

The attractive force of a mono-pole of magnet is written as follows:

$$f = \frac{A}{\mu_0} B^2 \tag{1}$$

where A is the air gap area, B is the flux density, μ_0 is the permeability. Equation (1) is rewitten as

$$f = \frac{A}{\mu_0} B^2 = \frac{A}{\mu_0}\left[\frac{N(i_0+i)}{\frac{l}{\mu}+\frac{x_0+x}{\mu_0}}\right]^2 \tag{2}$$

where i_0 is the bias current, x_0 is the steady-state gap length, x is the control gap, N is the number of winding turns, i is the control current, l is the flux length, μ is the permeability in the magnetic body. It is assumed that the steady-state attractive force is provided by the bias current of electromagnet.

Using the Taylor series expansion for small values of i and x, we can obtain the following attractive force with linear terms,

$$f_{(x,i)} = f_0 + \left|\frac{\partial f}{\partial x}\right|_{\substack{x=0\\ i=0}} x + \left|\frac{\partial f}{\partial i}\right|_{\substack{x=0\\ i=0}} i + \cdots \tag{3}$$

The second and the third terms show the first order purterbated attractive force in Eq.(3). The each coefficient is

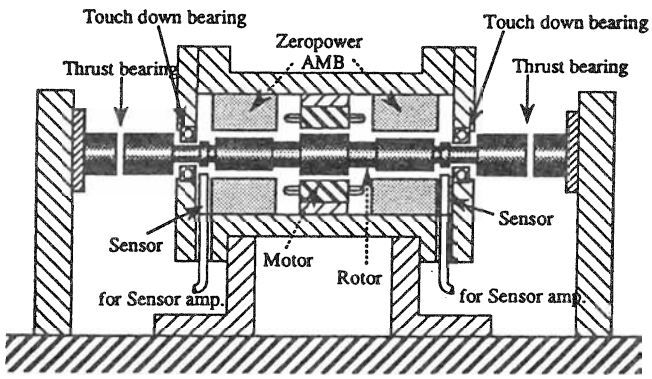

Fig. 3 Experimental setup of zero-power magnetic bearing system

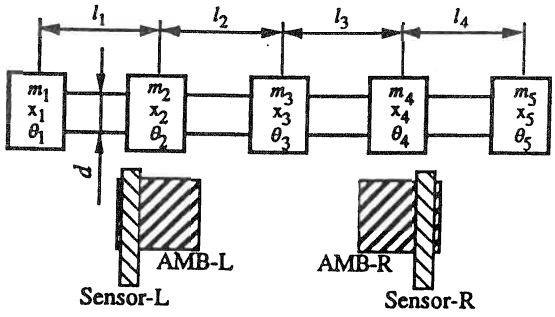

Fig. 4 Flexible rotor model using finite element method

given by

$$\left|\frac{\partial f}{\partial x}\right|_{\substack{x=0\\ i=0}} x = -k_1 x \ , \quad \left|\frac{\partial f}{\partial i}\right|_{\substack{x=0\\ i=0}} i = k_2 i \tag{4}$$

where

$$k_1 = \frac{2AN^2 i_0^{\,2}}{\mu_0^{\,2}(\frac{l}{\mu}+\frac{x_0}{\mu_0})^3} \ , \quad k_2 = \frac{2AN^2 i_0}{\mu_0(\frac{l}{\mu}+\frac{x_0}{\mu_0})^2}$$

The total attractive force is written by the first-order approximation as follows:

$$f \cong f_0 - k_1 x + k_2 i \tag{5}$$

Considering the pair of attractive forces, the magnetic force f due to the electromagnet along the radial direction can be modeled as the following equation:

$$f = f_1 - f_2 = -2k_1 x + 2k_2 i \tag{6}$$

The steady-state attractive force is supplied by a permanent magnet in the case of zero-power magnetic bearing, the coefficients in Eq.(6) are given as

$$k_1 = 2\frac{A}{\mu_0^{\,2}(\frac{l}{\mu}+\frac{x_0}{\mu_0})} B_{bias}^{\,2}, \ k_2 = 2\frac{AN}{\mu_0(\frac{l}{\mu}+\frac{x_0}{\mu_0})} B_{bias} \tag{7}$$

From Eq.(6),

$$f = -2k_1 x + 2k_2 i = -C_1 B_{bias}^{\,2} x + C_2 B_{bias} i \tag{8}$$

where

$$C_1 = \frac{4A}{\mu_0^{\,2}(\frac{l}{\mu}+\frac{x_0}{\mu_0})} \ , \quad C_2 = \frac{4AN}{\mu_0(\frac{l}{\mu}+\frac{x_0}{\mu_0})}$$

For simplicity, the following equation is used for control system design in this paper.

$$f = -4\frac{f_0}{x_0} x + 4\frac{f_0}{i_0} i \tag{9}$$

where

$$f_0 = \frac{A}{\mu_0} B_{bias}^2 \ , \quad B_{bias} = \frac{\mu_0 N i_0}{x_0}$$

It is assumed that $\frac{l}{\mu}+\frac{x_0}{\mu_0} \cong \frac{x_0}{\mu_0}$ because of $\frac{l}{\mu} << \frac{x_0}{\mu_0}$.

In this case, i_0 in Eq.(9) is used as an equivalent bias current to make a decision of a gain from coil curent to attractive force.

3.2 Modelin of Flexible Rotor

The free-free flexible rotor becomes the following equation of motion by the application of the finite element method (FEM):

$$M\ddot{q} + Kq = 0 \tag{10}$$

where $q = [\, q_1 \cdots q_5 \,]^T$, $q_i = [\, x_i \ \theta_i \,]$. when M denotes a mass matrix,K is the stiffness matrix, and q is the generalized displacement vector. The rotor is divided into four elements as shown in Fig.4. Table 1 shows the parameters used for modeling.

3.3 Modeling of Flexible Rotor / Zero-Power Magnetic Bearing

The flexible rotor shown in Fig.1 is restricted by the attractive forces given in Eq.(9). This resuts in

$$M\ddot{q} + Kq = Fp \tag{11}$$

where

$$F = \begin{bmatrix} 0&0&1&0&0&0&0&0&0&0 \\ 0&0&0&0&0&0&1&0&0&0 \end{bmatrix}^{\mathrm{T}}$$

$$p = \begin{bmatrix} p_1 x_2 - p_2 i_l \\ p_1 x_4 - p_2 i_r \end{bmatrix} \ p_1 = 4\frac{f_0}{x_0} \ , \ p_2 = 4\frac{f_0}{i_0}$$

The bias attractive forces and the control forces of Eq.(11) are separated as follows:

$$M\ddot{q} + K_1 q = F_1 u \tag{12}$$

where

$$u = [\, i_l \ i_r \,]^T \ , \ F_1 = -p_2 F \ , \ K_1 = K + K_p$$
$$K_p = \mathrm{diag}\,(-p_1, 0, 0, 0, 0, 0, 0, 0, -p_1, 0)$$

Using the modal analysis technique and selecting the normalized modal matrix Ψ and $q = \Psi\xi$, Eq.(12) is transformed to the form in modal coordinate as follows:

$$\ddot{\xi} + \Lambda\dot{\xi} + \Omega^2 \xi = F_0 u \tag{13}$$

where

$$I = \Psi^{\mathrm{T}} M \Psi, \ \Omega^2 = \Psi^{\mathrm{T}} K \Psi$$
$$\Lambda = 2\zeta\Omega, \ F_0 = \Psi^{\mathrm{T}} F_1$$

where Λ is the damping matrix. The damping ratio is determined experimentally. The state equation of the electromagnetic-mechanical system is given by

$$\begin{aligned} \dot{x}_f &= A_f x_f + B_f u \\ y &= C_f x_f \end{aligned} \tag{14}$$

where

$$A_f = \begin{bmatrix} 0 & I \\ -\Omega^2 & -\Lambda \end{bmatrix} \ , \quad B_f = \begin{bmatrix} 0 \\ F_0 \end{bmatrix} \ , \quad x_f = \begin{bmatrix} \xi^{\mathrm{T}} & \dot{\xi}^{\mathrm{T}} \end{bmatrix}^{\mathrm{T}}$$

$$C_f = \begin{bmatrix} C_0 \Psi & 0 \end{bmatrix} \ , \quad C_0 = \begin{bmatrix} 0&0&1&0&0&0&0&0&0&0 \\ 0&0&0&0&0&0&1&0&0&0 \end{bmatrix}$$

Because this MIMO system is originally unstable in an open loop, the control objective is to levitate the rotor and maintain the stability. In this case, there are only two unstable rigid mode, and the flexible modes are essentially stable, It is complicated to design a controller including full-order models for this high-order flexible system. Therefore, the construction of the reduced-order model is considered from the stand-point of stabilizing the two rigid modes and controlling the vibration of flexible modes. The reduced-order model is constructed by trancation of the higher-order modes in modal coordinates. Here, the state equation and the output equation covering as far as the second order mode which means only rigid modes are written as follows:

$$\begin{aligned} \dot{x}_r &= A_r x_r + B_r u \\ y &= C_r x_r \end{aligned} \tag{15}$$

where

$$x_r = [\, \xi_1 \ \xi_2 \ \dot{\xi}_1 \ \dot{\xi}_2 \,]^{\mathrm{T}} \qquad y = [\, x_2 \ x_4 \,]^{\mathrm{T}}$$
$$x_r \in R^4 \ \ u \in R^2 \ \ y \in R^2$$

4 PID Control for Zero-Power Magnetic Bearing System

First of all, we designed the analog PID control system to compare with a discrete time sliding mode control considering the performance. The design center (CAE software for electronic circuit simulator) was used for PID controller design. Figure 5 shows the step response at lift-off. The main purpose of this research is to save the electric power supply. It is necessary for full active magnetic bearing without permanent magnet to supply the total current 8A for levitation. On the other hand, it is enough for zero-power magnetic bearing system to supply the total current 1A. It is found that a zero-power magnetic bearing system can drastically save an energy.

5 Design of Discrete Time Sliding Mode Control System

5.1 Design of Hyperplane for Discrete Time System

This section will discuss the design of the digital controller. As a limitation of the structure, this magnetic bearing system has only two output feedbacks which can be measured directly. Therfore, the adaptive variable structure system (VSS) observer is used for system state estimation. Considering the reduced-order model system given in Eq.(15), the equivalent discrete-time system is found as

$$\begin{aligned} x_r(k+1) &= \Phi x_r(k) + \Gamma u(k) \\ y(k) &= C_r x_r(k) \end{aligned} \tag{16}$$

The switching function is defined by

$$\sigma(k) = S_d x_r(k) \tag{17}$$

The following equation is obtained when the system is in sliding mode,

$$\sigma(k) = \sigma(k+1) = \sigma(k+2) = \cdots \tag{18}$$

The equivalent control input is written from Eqs.(16),(17) and (18) as follows:

$$u_{eq}(k) = -(S_d\Gamma)^{-1} S_d(\Phi - I) x_r(k) \tag{19}$$

Substituting Eq.(19) into Eq.(16), we have the equivalent control system as follows:

$$x_r(k+1) = \left\{ \Phi - \Gamma(S\Gamma)^{-1} S_d(\Phi - I) \right\} x_r(k) \tag{20}$$

We choose the (n-m) closed loop eigenvalues of Eq.(20) so that they lie within the unit circle. These eigenvalues correspond to the (n-m) nonzero eigenvalues of the equivalent system. In this paper, the stability-degree specification method is applied in order to stabilize Eq.(20). The system matrix A_r with stability-degree specification is rewritten by

$$A_\varepsilon = A_r + \varepsilon I \tag{21}$$

S_d in Eq.(20) is obtained as follows:

$$S_d^{\mathrm{T}} = (R + \Gamma^{\mathrm{T}} P_d \Gamma)^{-1} \Gamma^{\mathrm{T}} P_d \Phi_\varepsilon \tag{22}$$

where P_d is the solution matrix of discrete time Riccati equation for the positive definite matrices Q, R as follows:

$$P_d - \Phi_\varepsilon^{\mathrm{T}} P_d \Phi_\varepsilon + \Phi_\varepsilon^{\mathrm{T}} P_d \Gamma (R + \Gamma^{\mathrm{T}} P_d \Gamma) \Gamma P_d^{\mathrm{T}} \Phi_\varepsilon - Q = 0$$

5.2 Design of Sliding Mode Controller

After the design of the switching surface, the next important aspect of VSS is guaranteeing the existence of the sliding mode. The variable structure system can be thought of as a closed-loop system with an adaptively varying state feedback gain. Therefore, the type of control law considered here consists of two independent functions: a linear state feedback control function u_L and nonlinear control function u_{NL}:

$$\left\{ \begin{aligned} u(k) &= u_L(k) + u_{NL}(k) \\ u_L(k) &= K_s x_r(k) = u_{eq}(k) \\ u_{NL}(k) &= -\alpha(k)\,\mathrm{sgn}[\,\sigma(k)\,] \end{aligned} \right\} \tag{23}$$

where

$$K_s = -(S_d\Gamma)^{-1} S_d(\Phi - I)$$

We proposed the VSS controller design without chattering[10],[11]. The conditions without chattering is to satisfy the following inequality for the switching functions $\sigma(k)$ and $\sigma(k+1)$.

$$\begin{aligned} &0 \le \sigma(k+1) < \sigma(k) \quad \sigma(k) > 0 \\ &\sigma(k) < \sigma(k+1) \le 0 \quad \sigma(k) < 0 \end{aligned} \tag{24}$$

The control input (23) is designed so that $\alpha(k)$ in Eq.(23) satisfies the inequality (24). From $\sigma(k+1) = S_d x_r(k+1)$,

$$\sigma(k+1) = S_d\left\{ \Phi x_r(k) + \Gamma(u_L(k) + u_{NL}(k)) \right\} \tag{25}$$

Substituting Eq.(20) and Eq.(23) into Eq.(24),

$$\sigma(k+1) = \sigma(k) - S_d\Gamma u_{NL}(k) \tag{26}$$

The condition to satisfy Eq.(24) is given by Eqs.(26),(24) as follows:

$$\sigma(k+1) \le \sigma(k) - S_d\Gamma\alpha(k) \tag{27}$$

Therefore, we obtain $\left\| S_d\Gamma \right| \alpha(k) \le \sigma(k)$. In same manner,

$$\sigma(k+1) \ge \sigma(k) - S_d\Gamma\alpha(k) \tag{28}$$

So, we have $\left| S_d\Gamma \right| \alpha(k) \le \left| \sigma(k) \right|$. Finally, the follwing expression is gotten.

$$\alpha(k) = \eta \frac{\left| \sigma(k) \right|}{\left| S_d\Gamma \right|} \tag{29}$$

The nonlinear control input without chattering is

$$u_{NL}(k) = -\eta \frac{\left| \sigma(k) \right|}{\left| S_d\Gamma \right|} \mathrm{sgn}[\,\sigma(k)\,] \tag{30}$$

where $0 < \eta \le 1$, $\sigma(k+1)\sigma(k) > 0$. Equation (30) is rewritten as follows:

$$u_{NL}(k) = -\eta \frac{\sigma(k)}{\left| S_d\Gamma \right|} \tag{31}$$

5.3 Design of Discrete Time VSS Observer

It is necessary for sliding mode control to obtain every state variable in general. We need a state observer to estimate for unmeasured state variables. The discrete time VSS observer as sliding mode observer is applied because the system has some disturbances and some uncertainty.

Since the system is observable, the all eigenvalues of the following equation Φ_0 can be placed within a unit circle using the matrix K_0.

$$\Phi_0 = \Phi - K_0 C_r \tag{32}$$

Here we applied an discrete time optimal control theory for design of K_0. The discrete time VSS observer is defined by

$$\hat{x}(k+1) = \Phi_0 \hat{x}(k) + K_0 y(k) + M(\tilde{y}) + \Gamma u(k) \tag{33}$$

where

$$\begin{aligned} \tilde{y}(k) &= y(k) - \hat{y}(k) = y(k) - C_r\hat{x}(k) \\ M(\tilde{y}) &= -\Gamma \frac{\tilde{y}(k)}{\left| \tilde{y}(k) \right| + \gamma} \rho \end{aligned}$$

5.4 Stability of Sliding Mode Control System with VSS Observer

Each sliding mode control system as a regurator and sliding mode observer as a estimator must be stable respectively. However, the total stability including a regulator and a estimator is not guaranteed. So, we consider the whole stability of closed loop system with the sliding mode control system and the VSS observer system.

The discrete time sliding mode controller and the discrete time VSS observer are shown in Eq.(23) and Eq.(33). It is very difficult to analyze the characteristics because these equations include nonlinear term. Therefore, we assume that the regulator and the observer are on the hyperplane as sliding mode. We discuss the closed loop stability of such case regarding as the equivalent control system. Equations (23) and (33) yield the following form.

$$u(k) = u_L(k) = K_s\hat{x}(k) \tag{34}$$

$$\hat{x}(k+1) = \Phi_0\hat{x}(k) + K_0 y(k) + \Gamma u(k) \tag{35}$$

Equations (16),(34) and (35) are combined as follows:

$$\begin{bmatrix} x_r(k+1) \\ \hat{x}(k+1) \end{bmatrix} = \begin{bmatrix} \Phi & -\Gamma(S_d\Gamma)^{-1} S_d(\Phi - I) \\ K_0 C_r & \Phi_0 + \Gamma(S_d\Gamma)^{-1} S_d(\Phi - I) \end{bmatrix} \begin{bmatrix} x_r(k) \\ \hat{x}(k) \end{bmatrix} \tag{36}$$

If the whole eigenvalues except the number of control inputs are stable, the closed-loop system becomes stable on the condition every state variable is constraint in sliding mode. In the same manner, this approach is used for a full-order model with the truncation modes. The full-order model is defined by

$$x_f(k+1) = \Phi_f x_f(k) + \Gamma_f u(k)$$
$$y(k) = C_f x_f(k) \tag{37}$$

Using Eq.(37), we have the following equation taking into account the higher-order modes.

$$\begin{bmatrix} x_f(k+1) \\ \hat{x}(k+1) \end{bmatrix} = \begin{bmatrix} \Phi_f & -\Gamma_f (S_d \Gamma)^{-1} S_d (\Phi - I) \\ K_0 C_f & \Phi_0 + \Gamma (S_d \Gamma)^{-1} S_d (\Phi - I) \end{bmatrix} \begin{bmatrix} x_f(k) \\ \hat{x}(k) \end{bmatrix} \tag{38}$$

In the case that Eq.(38) could be stable, the sliding mode control system with the sliding mode observer has a strong robustness. It is very important to determine the matices S_d, K_0 to stabilize Eq.(38).

6 Simulations and Experiments of Discrete Time Sliding Mode Control

6.1 Simulations at lift-off

Table 2 shows the parameters used in the simulations. Figure 6 shows the block diagram of discrete time sliding mode control. The sampling time of discrete time sliding mode controller was 400 μsec. The step response at lift-off using discrete time sliding mode control. It is found that the performanes of Fig.7 is excellent and superior to PID control.

6.2 Experiments

Figure 8 shows the schematic diagram of experiments. Figure 9 shows the step response at lift-off. It seems that the spillover phenomena occur from Fig.9. However, the system does not become unstable. We ran up the rotational speed up to 4500 rpm successufully. Figure 10 shows the shaft vibration at 4500 rpm. It was impossible to increse a rotational speed up to 4500 rpm for the analog PID control because of big unbalance mass. However, the rotor can pass through the rigid critical speed with small vibration in discrete time sliding mode control. It was impossible to run up to higher rotational speed because of a brake torque caused by eddy current. We have been trying to build up a new rotor which means a laminated rotor to reduce eddy current loss.

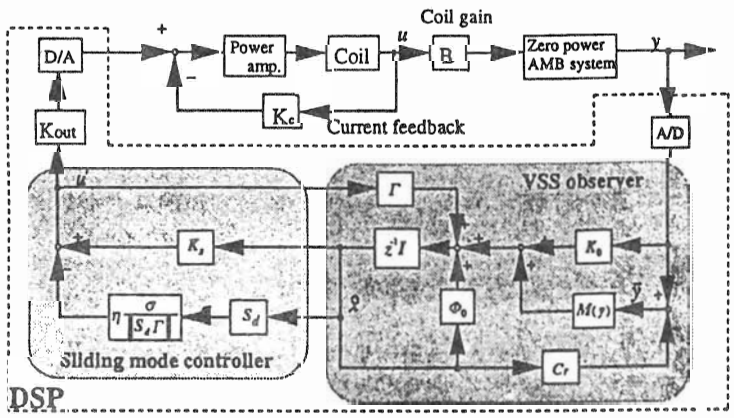

Fig. 10 Block diagram of discrete time sliding mode control

Table 1 Parameter of Fig. 4

m_1	0.260 kg	l_1	68.00 mm
m_2	0.374	l_1	92.00
m_3	0.100	l_1	92.00
m_4	0.374	l_1	68.00
m_5	0.260	d	13.95

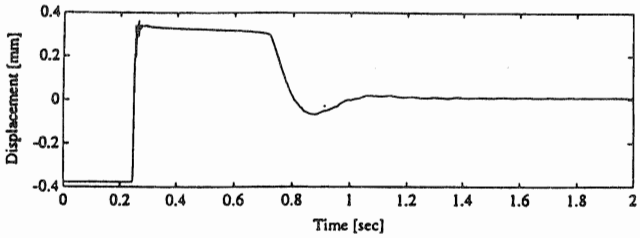

Fig. 7 Step response at lift-off using PID analog controller

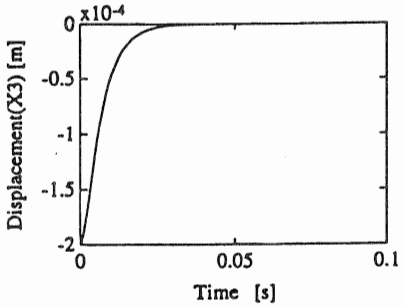

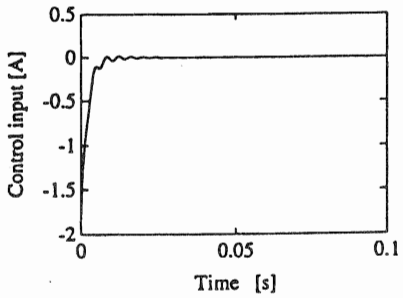

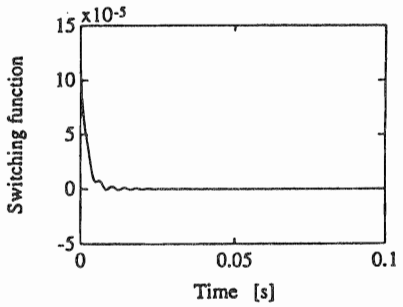

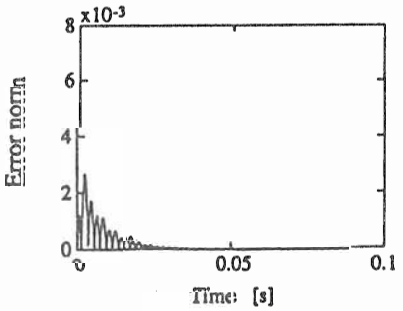

Fig. 11 Step response at lift-off using discrete time sliding mode control (Computed)

Table 2 Parameter used for control system design

Controller		Observer		Model	
ε	15	ρ	10	f_0	4 N
δ	0.002	γ	0.005	i_0	1.3 A
φ	10000	Q	$\begin{bmatrix} 10 & & 0 \\ & 10^5 & \\ 0 & & 10^5 \end{bmatrix}$	x_0	0.0005 m
η	0.2				
Q	I_{4x4}				
R	I_{2x2}	R	I_{2x2}		

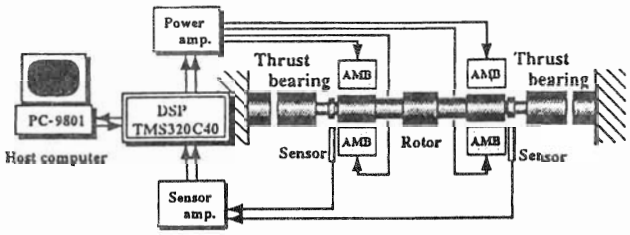

Fig. 12 Schematic diagram of experimental setup

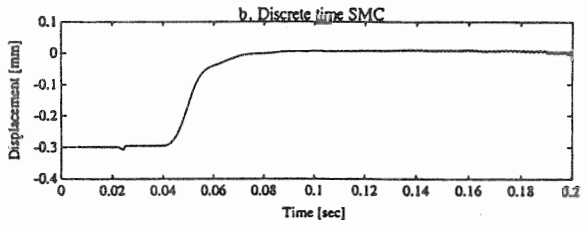

Fig. 13 Step response at lift-off using discrete time sliding mode control (Experimental)

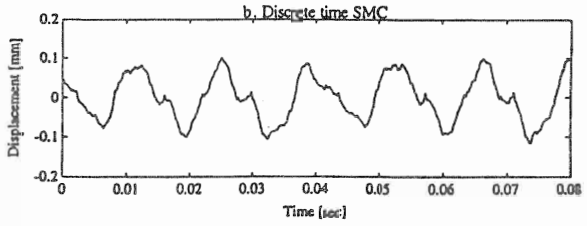

Fig. 14 Experimental result of time history response at 4 500 rpm with discrete time sliding mode control

6 Conclusions

We proposed a new zero-power magnetic bearing with variable attractive force of permanent magnet. Also, we designed a discrete time sliding mode control system using the proposed convenient and simple discrete time sliding mode control system design scheme. The conclusions are summarized as follows:

(1) We proposed a new zero-power magnetic bearing with variable attractive force of permanent magnet. It is very easy to tune a control system.

(2) We carried out the modelling for a zero-power magnetic bearing system. The common and different points were made clear.

(3) It was made sure that the discrete time sliding mode control is superior to conventional a PID control.

(4) It is very useful for a zero-power magnetic bearing system proposed in this paper to save a energy. It is hoped that such magnetic bearings will be applied in future.

References

(1)G.Schweitzer (edited), Proc.of the 1st International Symposium on Magnetic Bearings,1988

(2)T.Higuchi (edited), Proc.of the 2nd International Symposium on Magnetic Bearings,1990

(3)P.Allair (edited), Proc.of the 3rd International Symposium on Magnetic Bearings,1992

(4)G.Schweitzer (edited), Proc.of the 4th International Symposium on Magnetic Bearings,1994

(5)K.Nonami,H.Ueyama and Y.Segawa, H_∞ Control of Milling AMB Spindle, JSME International Journal, 39-3, 1996, to appear

[6]K. Nonami and T.Ito, μ Synthesis of Flexible Rotor Bearing Systems, IEEE Trans. on Control System Technology, Special Issue on Magnetic Bearings, 1996, to appear

[7]N.Ide, K.Nonami and H.Ueyama, Robust Control of Magnetic Bearing Systems Using μ Synthesis with Discriptor Form, Proc of the 3rd Motion and Vibration Control, 1996, to appear

[8]S.Sivrioglu and K.Nonami, LMI Based Gain Scheduled H_∞ Controller Design for AMB Systems under Gyroscopic and Unbalance Disturbance Effect, Proc.of the 5th International Symposium on Magnetic Bearings,1996

[9]S.Sivrioglu and K.Nonami, Advanced Mixed H_2/H_∞ Control Design for Active Magnetic Bearing Systems, Proc.of the 5th International Symposium on Magnetic Bearings,1996

[10]H.Tian and K.Nonami, Robust Control of Flexible Rotor-Magnetic Bearing Systems Using Discrete Time Sliding Mode Control, JSME International Journal, Ser.C, 37-3, 504-512, 1994

[11]K.Nonami and H.Tian, Sliding Mode Control, Corona Pub., 1994